PL-TR-97-2158

REGIONAL WAVE PROPAGATION CHARACTERISTICS IN SOUTHERN ASIA

Richard Rapine
Chris Reese
James Ni
Tom Hearn

New Mexico State University
Department of Physics
Las Cruces, NM 88003-8001

31 October 1997

Final Report
1 November 1995 - 31 October 1997

Approved for public release; distribution unlimited

DEPARTMENT OF ENERGY
Office of Non-Proliferation
and National Security
WASHINGTON, DC 20585

AIR FORCE RESEARCH LABORATORY
Space Vehicles Directorate
29 Randolph Road
AIR FORCE MATERIEL COMMAND
HANSCOM AFB, MA 01731-3010

SPONSORED BY
Department of Energy
Office of Non-Proliferation and National Security

MONITORED BY
Air Force Research Laboratory
CONTRACT No. F19628-95-K-0009

The views and conclusions contained in this document are those of the authors and should not be interpreted as representing the official policies, either express or implied, of the Air Force or U.S. Government.

This technical report has been reviewed and is approved for publication.

Katharine Kadinsky-Cade
KATHARINE KADINSKY-CADE
Contract Manager

CHARLES P. PIKE, Deputy Director
Integration and Operations Division

This report has been reviewed by the ESD Public Affairs Office (PA) and is releasable to the National Technical Information Service (NTIS).

Qualified requestors may obtain copies from the Defense Technical Information Center. All others should apply to the National Technical Information Service.

If your address has changed, or you wish to be removed from the mailing list, or if the addressee is no longer employed by your organization, please notify AFRL/VSOS-IM, 29 Randolph Road, Hanscom AFB, MA 01731-3010. This will assist us in maintaining a current mailing list.

Do not return copies of the report unless contractual obligations or notices on a specific document requires that it be returned.

REPORT DOCUMENTATION PAGE

Form Approved
OMB No. 0704-0188

1. AGENCY USE ONLY *(Leave blank)*	2. REPORT DATE	3. REPORT TYPE AND DATES COVERED
	31 October 1997	Final Report (1 Nov 95-31 Oct 97)

4. TITLE AND SUBTITLE

Regional Wave Propagation Characteristics in Southern Asia

5. FUNDING NUMBERS

F19628-95-K-0009
PE 69120H
PR DENN TA GM
WU AH

6. AUTHOR(S)

Richard Rapine, Chris Reese, James Ni and Thomas Hearn

7. PERFORMING ORGANIZATION NAMES(S) AND ADDRESS(ES)

New Mexico State University
Department of Physics
Las Cruces, NM 88003-8001

8. PERFORMING ORGANIZATION REPORT NUMBER

9. SPONSORING / MONITORING AGENCY NAMES(S) AND ADDRESS(ES)

Air Force Research Laboratory
29 Randolph Road
Hanscom AFB, MA 01731-3010
Contract Manager: Katherine Kadinsky-Cade/vSBS

10. SPONSORING / MONITORING AGENCY REPORT NUMBER

PL-TR-97-2158

11. SUPPLEMENTARY NOTES

This research was sponsored by Department of Energy, Office of Non-Proliferation & National Security, Washington, D.C. 20585

a. DISTRIBUTION / AVAILABILITY STATEMENT

Approved for public release; distribution unlimited.

12. DISTRIBUTION CODE

13. ABSTRACT *(Maximum 200 words)*

Lg Q values were determined for most parts of China. Higher Q values are seen from paths crossing the Tarim Platform. Lower Q values are found in Burma, southern Tibet, and along the mountains that border the eastern Tibetan Plateau. The overall low Q values found in China are similar to Q values found in the western United States. Large north-south variations were observed for the attenuation of the regional phases Pn and Lg at the CDSN station LSA. These variations reflect the rheological properties of the uppermost mantle and the crust, respectively.

14. SUBJECT TERMS	15. NUMBER OF PAGES
Crustal structure, Seismic studies, Southern Asia, Tibetan Plateau	44
	16. PRICE CODE

17. SECURITY CLASSIFICATION OF REPORT	18. SECURITY CLASSIFICATION OF THIS PAGE	19. SECURITY CLASSIFICATION OF ABSTRACT	20. LIMITATION OF ABSTRACT
Unclassified	Unclassified	Unclassified	SAR

Table of Contents

List of Illustrations

Part II

List of Tables

Part I: Lg attenuation coefficients in China and surrounding regions

1.1 Introduction

At regional distances along continental paths, seismograms are characterized by Pn, Pg, Sn and Lg phases. Lg often has the largest amplitude coda signal for stable continental paths. Lg has been modeled successfully as a sum of higher-mode surface waves with an approximate group velocity of 3.5 km/s (Knopoff et al., 1973). Since the amplitude of the Lg wave is related to crustal attenuation and scattering, its amplitude has been used to estimate the value of crustal Q (e.g., Herrmann, 1980; Shin and Herrmann, 1987). For the tectonically active western United States, Lg Q lies within the range between 140 and 300. Low Lg Q was also found on the Turkish-Iranian Plateau by Nuttli (1980) and Wu et al. (1996). In contrast, the eastern United States and Canada have higher Lg Q values of about 1000. These results indicate that there exists a strong positive correlation between Lg Q and regional tectonic activity.

The unique properties of Lg make it useful for estimating event magnitudes and yield estimates for explosions. In stable continental and shield regions, large Lg amplitudes can be seen at large distances because of the low anelastic attenuation in these regions. Thus, it is believed that Lg has the potential for yield estimation with high accuracy. Nuttli (1986) and Patton (1988) obtained yield estimates of Nevada Test Site (NTS) explosions using Lg wave amplitudes. Hansen et al. (1990) used regional Lg phases recorded at a single station to estimate source size. They found a very small scatter in the plot of m_b versus RMS Lg amplitudes and indicated that Lg amplitudes give a reliable estimate of the relative magnitude of a nuclear explosion. However, due to the various attenuation properties associated with variations in geologic, tectonic and topographic structure, it is necessary to develop an empirical basis to allow for correction of attenuation of the Lg phase.

1.2 Data

Regional network data from the CDSN (Chinese Digital Seismic Network) and from IRIS (Incorporated Research Institutions for Seismology) stations were retrieved from the IRIS-DMC

(Data Management Center). Location information for these stations is listed in Table 1 and is depicted on a map in Figure 1. All stations contained three component broadband sensors recording in triggered mode at 20 samples per second. This data set consisted of seismic events with body wave magnitudes greater than 4.3, focal depths less than 50 km and epicentral distances between 500 and 1500 km. Event locations and origin times were taken from the PDE (Preliminary Determination of Epicenters) catalogs. Lg propagation efficiencies of the data were already characterized in a previous study by Rapine et al. (1997) as efficient, inefficient and blocked. To help separate anelastic attenuation from scattering attenuation in the crust, only efficient Lg waves were used. The data were further constrained by choosing only those earthquakes lying within a certain back azimuth around each station.

1.3 Method

The amplitude of Lg is defined in several different ways. Nuttli (1980) defined the third highest peak in the Lg wave train as the Lg amplitude. Rodgers et al. (1997) used an envelope mean over the Lg time window as one method to obtain Lg amplitudes. This approach was used as a measure of the average Lg energy within the specified time window. Some studies have also defined the RMS (root mean square) amplitude over the Lg group velocity window as the Lg amplitude (e.g., Hansen et al., 1990; Rodgers et al., 1997). Hansen et al. (1990) showed that RMS Lg is a stable source size estimator and can be used to provide a reliable magnitude estimate. This study follows Hansen's method and defines the Lg amplitude as the maximum RMS amplitude in the Lg group velocity window. The RMS amplitude of the seismogram is computed within a moving window of width N and is calculated by

$$A_{RMS} = \left[\frac{1}{N}\sum s^2(i)\right]^{1/2} \tag{1}$$

where A(t) is the RMS amplitude at time t on the seismogram and s(i) is the signal measurement at time i in the time window. A 55-second time window was chosen because it corresponds to

Table 1. Broadband Station Locations

Station Name	Latitude (°N)	Longitude (°E)	Elevation (m)
WMQ	43.821	116.175	43
LSA	29.700	91.150	3789
KMI	25.123	102.740	1945
LZH	36.087	103.844	1560
CHTO	18.790	98.977	316

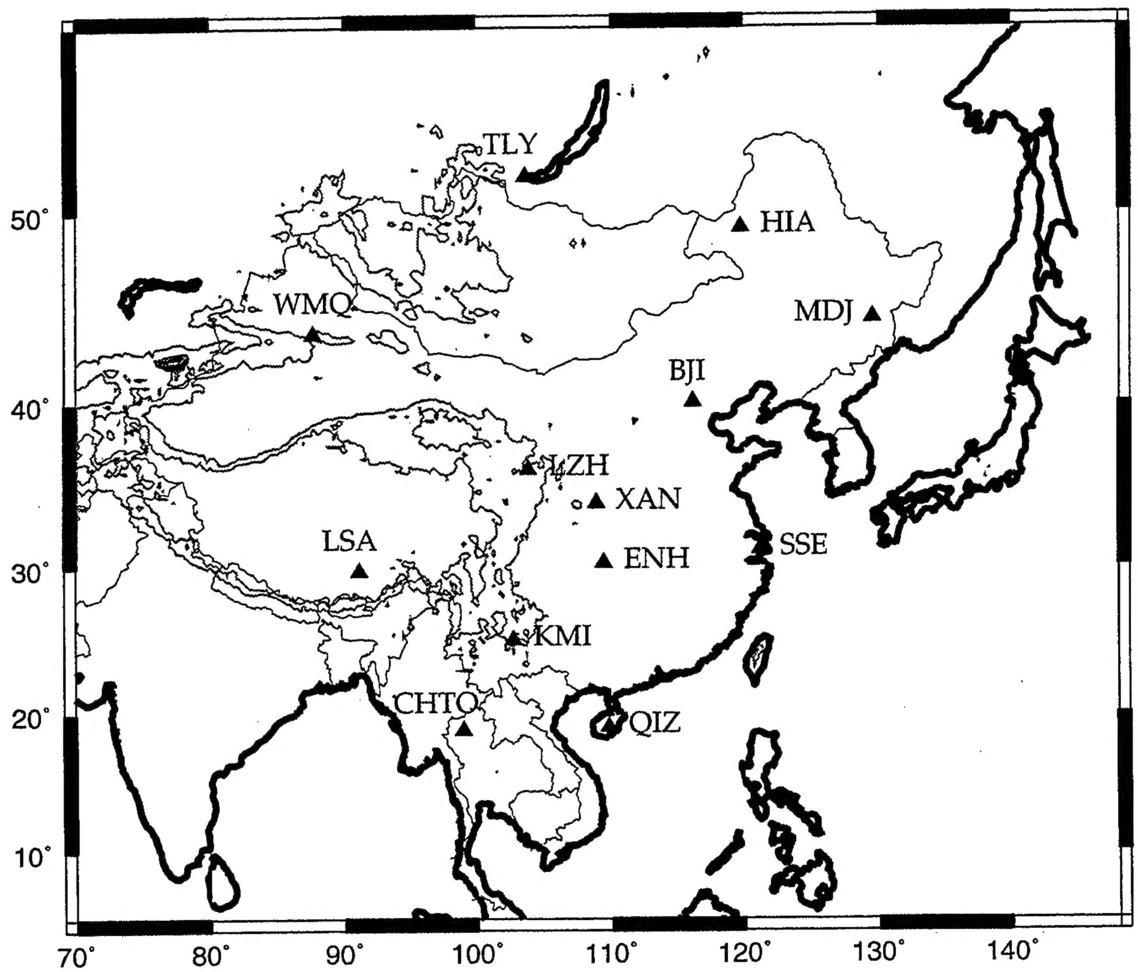

Figure 1. Station location map of IRIS and CDSN stations in eastern Asia. Triangles represent broadband station locations. Gray contour lines represent 2000 and 4000 m elevations.

the average time duration of Lg waves in the region. Hansen et al. (1990) showed that the length of the time window is not overly critical because of the robustness of the results. The data were also filtered between 0.5 - 5.0 Hz to enhance the main part of the Lg energy.

Attenuation of the vertical component Lg wave can be described by the relation

$$A(\Delta) = \frac{A_0 e^{-\gamma\Delta}}{(\sin\Delta)^{1/2}\Delta^{1/3}} \tag{2}$$

where $A(\Delta)$ is the RMS amplitude, Δ is the epicentral distance in km, A_0 is the initial amplitude, and γ is the anelastic attenuation coefficient (Ewing et al., 1957). The $(\sin \Delta)^{1/2}$ term corrects for geometrical spreading and the $\Delta^{1/3}$ term is the amplitude correction for dispersion in the time domain. The 1/3 exponent used here was shown by Campillo et al. (1985) to correspond to the Airy phase. All amplitudes were equalized to a m_b 5.0 earthquake by the formula

$$(\log_{10} A - \log_{10} A') = m_b - 5.0 \tag{3}$$

where A is the measured RMS Lg amplitude, A' is the equalized Lg amplitude, and m_b is the body wave magnitude given from the PDE catalogs. Nuttli (1980) explained that errors introduced by equalization would not change the results significantly. An error of 0.5 m_b would result in a multiplicative error of 3.2 in the equalized amplitude. The attenuation coefficient was calculated using a grid search method minimizing the L1 norm to estimate A_0 and γ. The curvature of the error surface was used to calculate the formal error of A_0 and γ (Menke, 1988). The attenuation coefficient, γ, is related to Q by $\gamma = (\pi f) / (QU)$ where f is the frequency and U is the Lg group velocity. The Lg frequency used in these calculations was 1 Hz with a group velocity of 3.5 km/s. The attenuation coefficients can then be used to determine Lg Q for the crust in eastern Asia.

1.4 Results

Figure 2 shows a map of event-station paths which were used to examine the propagation and attenuation characteristics of Lg. It is evident that Lg paths cross over different tectonic regions and thus, the attenuation properties will be different for some stations. Tables 2-6 list the events used to calculate attenuation coefficients around each station and provide origin times, event locations, distances, back azimuths, and body wave magnitudes. The Lg attenuation coefficient for paths across the Tarim Platform, southeast of station WMQ, is 0.0030 ± 0.0005 km^{-1} (Figure 3). This coefficient corresponds to a 1 Hz Lg Q value of 300 ± 50. Although this is one of the higher values we calculated, it is still low when compared to stable continental shields which have Q values over 1000. For 10 events from station LSA, the Lg attenuation coefficient is 0.0036 ± 0.0008 km^{-1} corresponding to a Q of 249 ± 55 (Figure 4). The attenuation coefficient for KMI is 0.0067 ± 0.0005 km^{-1} corresponding to a Q of 134 ± 9 (Figure 5). For propagation paths through the mountain fold belts along the eastern border of the Tibetan Plateau, the attenuation coefficient was found at LZH to be 0.0067 ± 0.0009 km^{-1} (Figure 6). This attenuation coefficient corresponds to a Lg Q value of 134 ± 18 at 1 Hz. This value is the same as that found near KMI. Lg is highly attenuated in Burma as evidenced by the high attenuation coefficient of 0.0106 ± 0.0013 km^{-1} corresponding to a Q of 85 ± 10 (Figure 7). Back-arc subduction and high heat flow are most likely the cause of the attenuated Lg amplitudes in Burma.

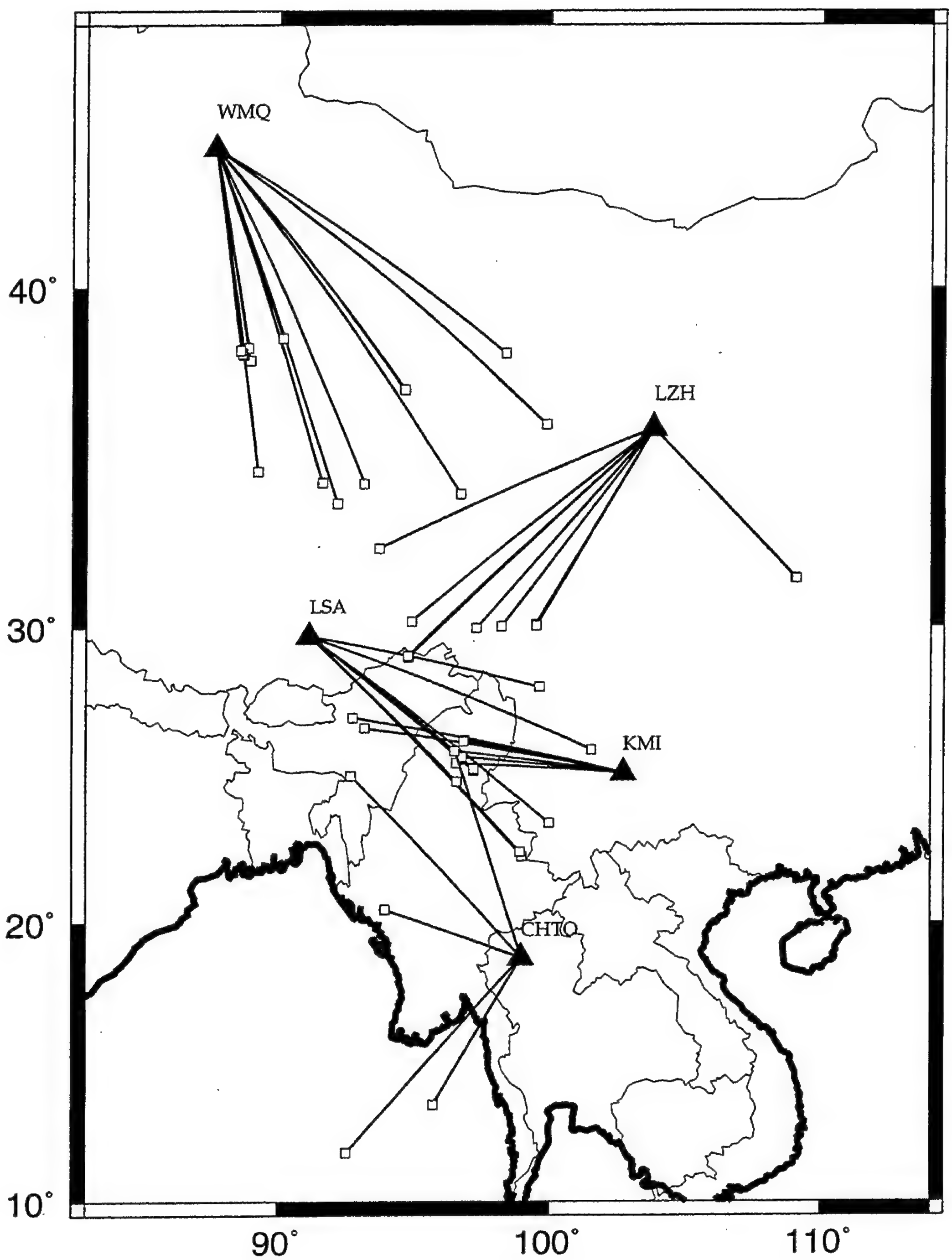

Figure 2. Map of station-event paths used for calculating attenuation coefficients for each station. Triangles represent station locations and squares represent event locations. Dark lines are the Lg paths.

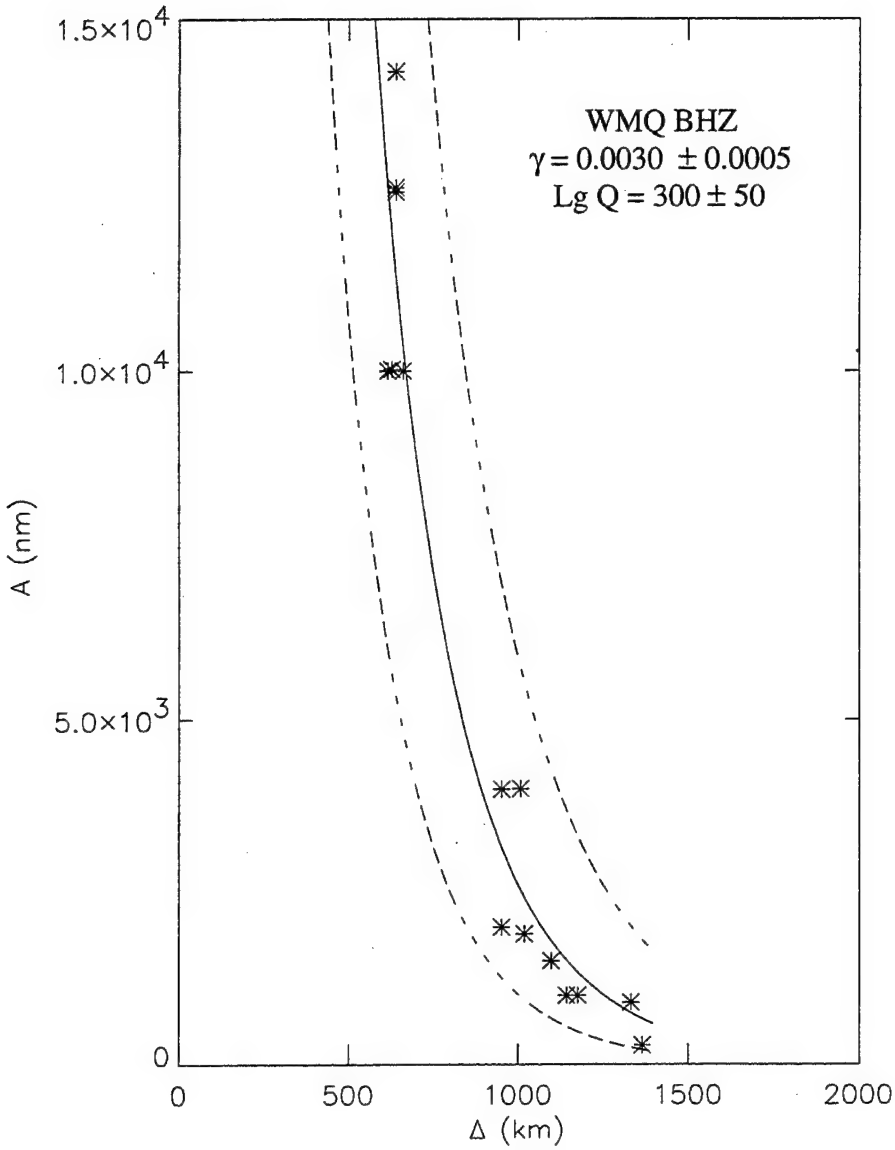

Figure 3. Lg attenuation curve for events around station WMQ for backazimuths between 135 and 180 degrees. The coefficient of attenuation, γ, and Lg Q value are listed inside the graph. The dashed lines represent one standard deviation from the best fit curve.

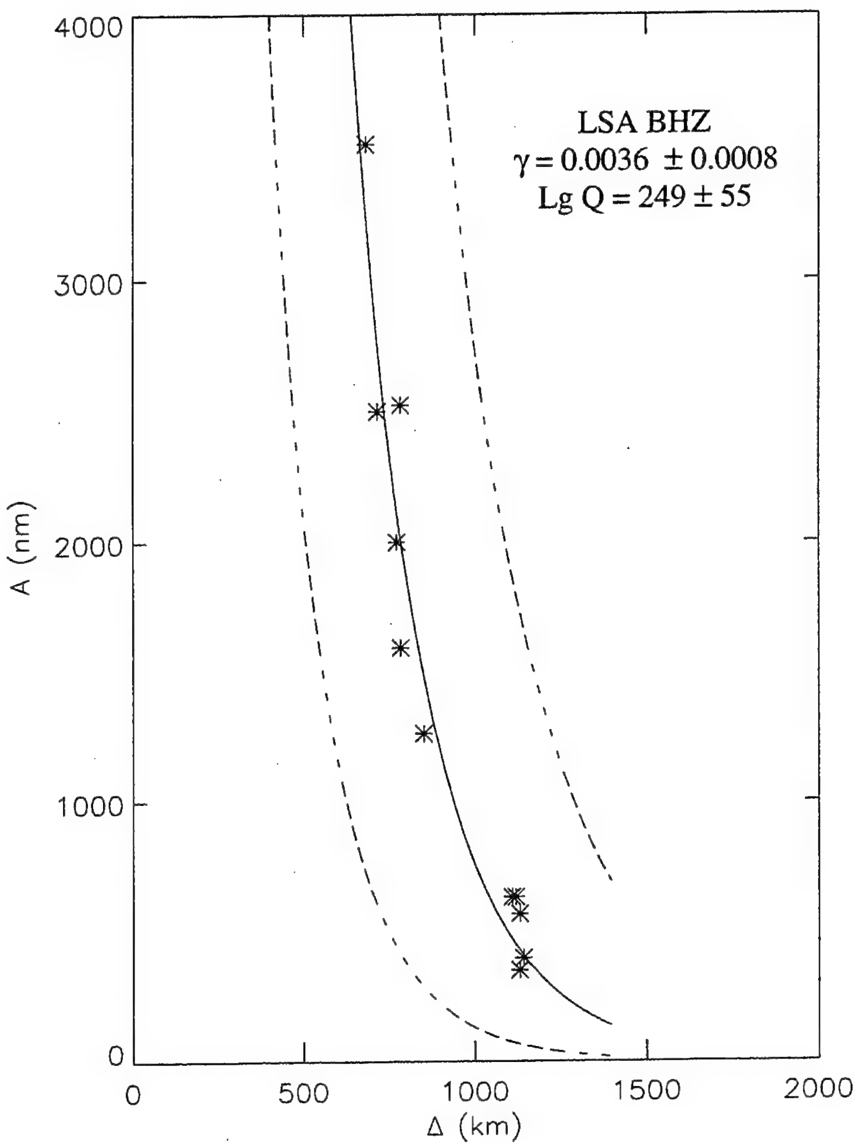

Figure 4. Lg attenuation curve for station LSA for events with backazimuths between 90 and 135 degrees.

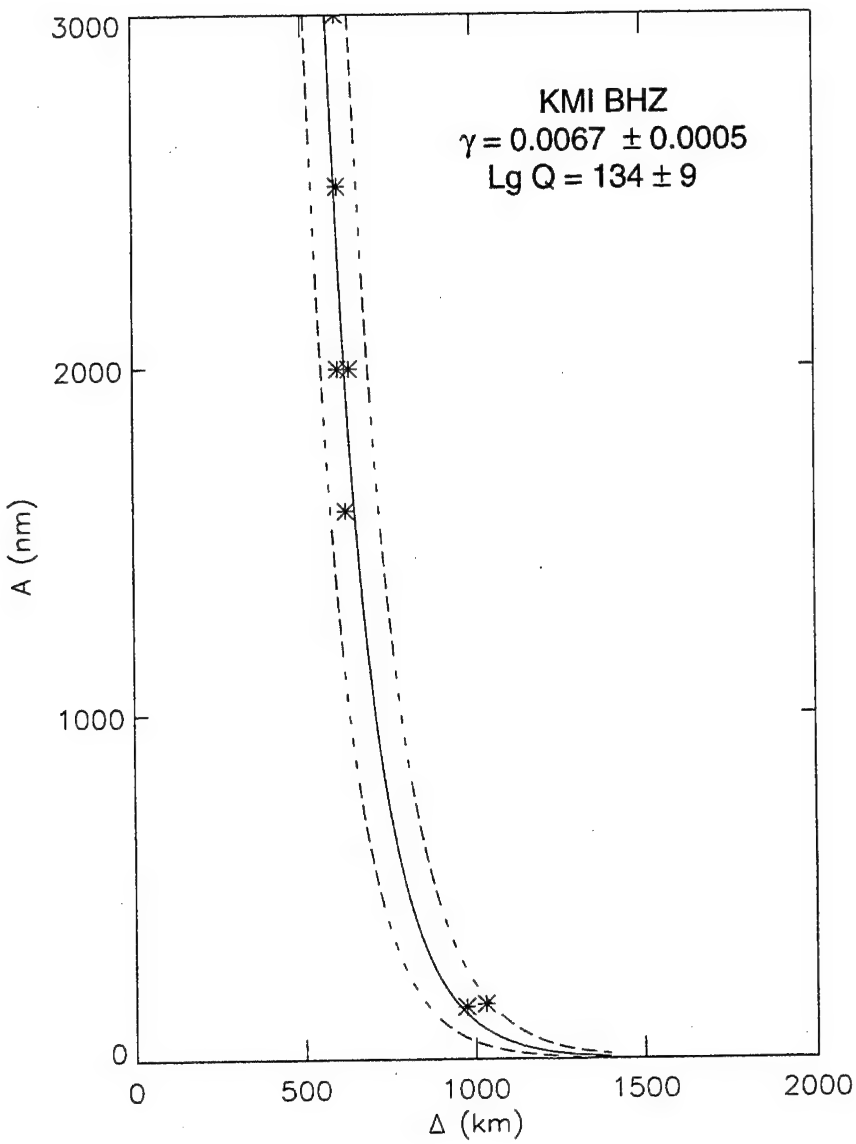

Figure 5. Lg attenuation curve for events around station KMI with backazimuths between 260 and 290 degrees.

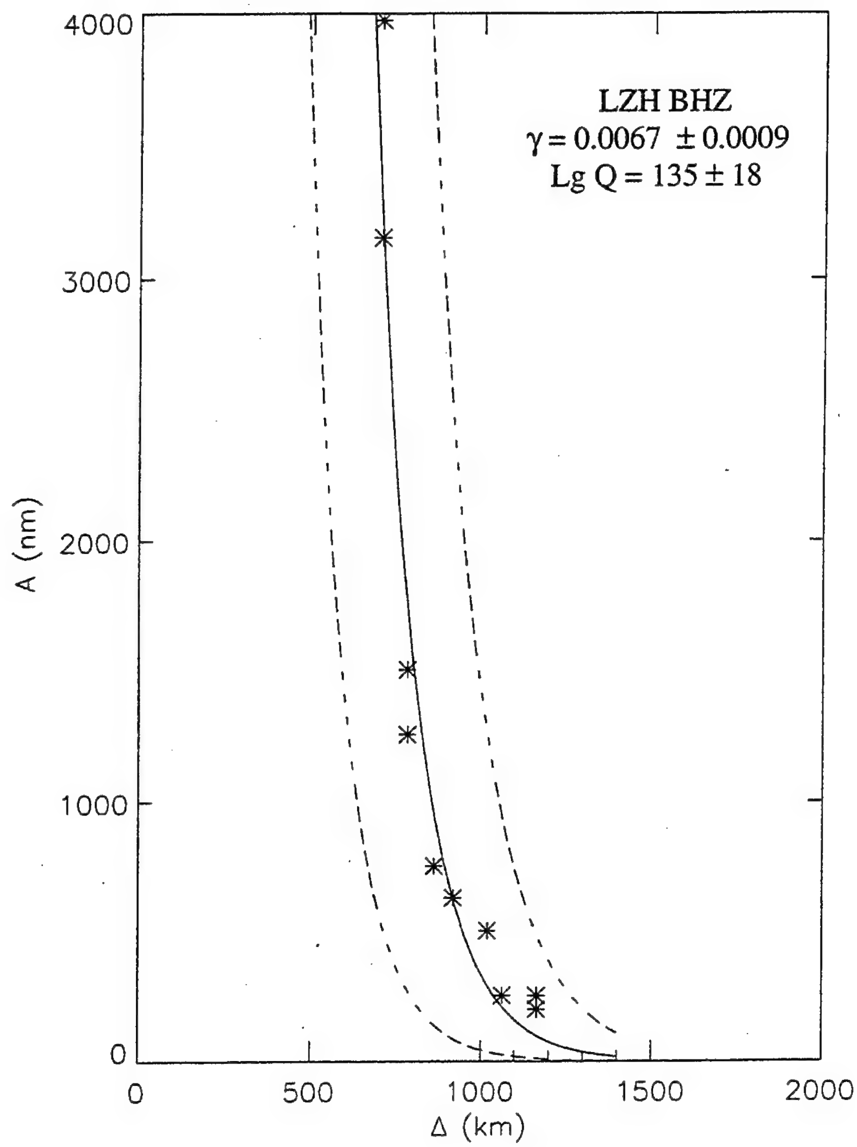

Figure 6. Lg attenuation curve for events around station LZH with backazimuths between 135 and 250 degrees.

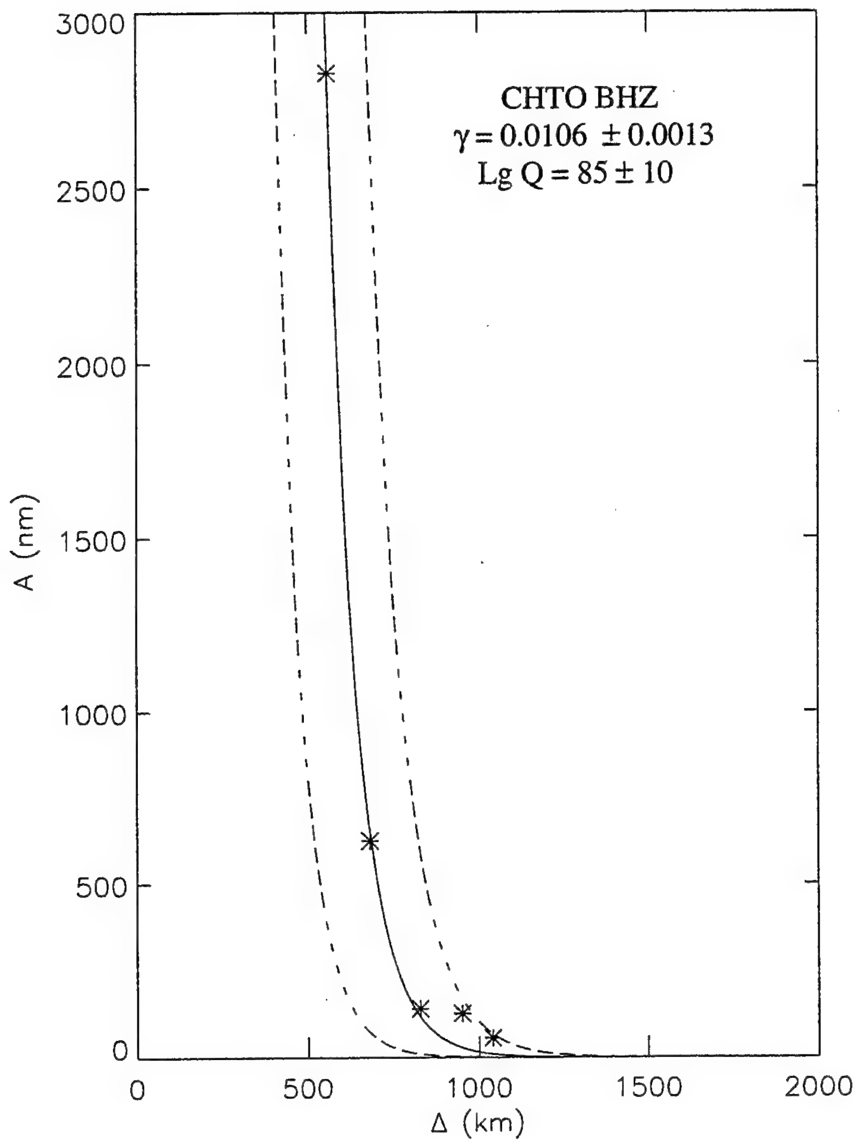

Figure 7. Lg attenuation curve for events around station CHTO for backazimuths between 210 and 340 degrees.

Table 2. Event Data Set for Station LZH

Date	Origin Time (UT)	Latitude (°N)	Longitude (°E)	Distance (km)	Baz (°)	m_b
01/25/88	01:12:21	30.18	94.89	1060	234	5.4
05/09/88	16:03:38	29.00	94.78	1157	230	5.1
05/10/88	20:51:40	29.05	94.77	1154	230	4.9
09/03/88	12:52:47	29.97	97.31	912	224	5.1
05/03/89	05:53:01	30.09	99.47	781	213	6.1
05/03/89	15:41:31	30.05	99.50	783	212	5.8
06/01/89	18:03:43	31.58	109.05	694	135	4.6
07/14/90	01:37:28	31.56	109.10	699	135	4.4
10/18/93	16:35:02	30.03	98.24	846	219	4.8
06/29/94	18:22:37	32.53	93.71	1010	250	5.8

Table 3. Event Data Set for Station LSA

Date	Origin Time (UT)	Latitude (°N)	Longitude (°E)	Distance (km)	Baz (°)	m_b
04/23/92	18:18:12	22.30	99.00	1135	135	4.8
04/28/92	21:03:04	22.43	98.93	1120	134	4.6
06/10/92	13:41:25	25.66	96.76	711	128	4.7
01/31/93	19:33:34	25.91	101.54	1104	110	4.9
04/02/93	21:09:52	24.82	96.58	762	134	4.4
06/03/93	01:15:37	23.42	100.00	1122	126	4.7
07/17/93	09:46:35	28.01	99.64	847	101	5.3
12/09/93	18:26:19	25.86	96.51	678	128	4.7
01/11/94	00:52:00	25.20	97.22	780	128	5.9
01/11/94	02:18:06	25.25	97.22	776	128	4.5

Table 4. Event Data Set for Station CHTO

Date	Origin Time (UT)	Latitude (°N)	Longitude (°E)	Distance (km)	Baz (°)	m_b
09/30/93	17:04:46	11.81	92.53	1038	223	5.4
12/09/93	18:26:19	25.86	96.51	825	342	4.7
05/29/94	14:35:54	20.45	93.94	558	290	4.7
07/24/94	23:39:07	25.04	92.68	950	318	4.7
11/22/94	15:38:35	13.56	95.72	677	211	4.9

Table 5. Event Data Set for Station WMQ

Date	Origin Time (UT)	Latitude (°N)	Longitude (°E)	Distance (km)	Baz (°)	m_b
04/13/89	02:07:89	34.18	96.71	1322	141	4.4
04/30/89	12:28:38	36.20	99.86	1335	125	4.8
09/19/90	08:05:57	38.00	88.94	655	170	4.4
02/26/91	15:38:42	34.54	91.61	1085	161	4.7
08/10/91	20:21:52	33.91	92.16	1167	159	4.7
02/03/92	15:44:23	34.50	93.15	1137	154	4.7
06/10/92	02:37:01	38.62	90.15	613	160	4.4
09/04/93	20:22:30	37.19	94.61	940	139	5.1
09/05/93	22:40:27	37.19	94.64	941	139	5.1
10/02/93	08:42:33	38.19	88.66	631	172	6.2
10/02/93	17:23:33	38.17	88.69	633	172	5.6
10/02/93	23:50:00	38.36	88.88	615	170	4.8
10/12/93	20:49:23	38.28	88.60	620	173	4.7
08/14/94	07:38:28	34.87	89.23	1003	172	4.4
08/27/94	07:41:42	38.20	98.36	1089	121	4.7

Table 6. Event Data Set for Station KMI

Date	Origin Time (UT)	Latitude (°N)	Longitude (°E)	Distance (km)	Baz (°)	m_b
02/12/89	07:55:48	26.22	96.87	600	283	5.0
03/08/89	20:02:04	26.99	92.75	1018	284	5.1
03/08/89	18:57:01	25.45	95.56	622	275	4.8
06/23/91	10:04:00	26.64	93.19	969	282	5.3
06/10/92	13:41:25	25.66	96.76	603	277	4.7
12/09/93	18:26:19	25.86	96.51	630	279	4.7
04/06/94	07:03:28	26.19	96.84	603	283	5.6

1.5 Conclusion

High quality digital data were obtained from stations located in China and its surrounding regions. Lg wave attenuation is estimated from these data for continental paths around CDSN and IRIS stations. Lg attenuation coefficients are calculated from RMS vertical component amplitudes and are used to determine Lg Q values for the crust in China. The Q values of 1 Hz Lg waves vary from approximately 100 to 300 for the stations under investigation here. Higher Q values are seen from paths crossing the Tarim Platform. Lower Q values are found in Burma, southern Tibet, and along the mountain fold belts that border the eastern Tibetan Plateau. The overall low Q values found in China are similar to Q values found in the western United States and the Iranian Plateau and could correspond to a similarity in the tectonic history of these regions. The calculated attenuation coefficients will be helpful in creating regional magnitude formulas for China and its surrounding regions. Lg amplitudes and a knowledge of the attenuation of Lg can also be used to estimate yield size of nuclear explosions in the region. These results will be useful for monitoring a nuclear test ban treaty.

1.6 References

Campillo, M., J. Plantet, and M. Bouchon (1985). Frequency-dependent Attenuation in the crust beneath Central France from Lg Waves: Data Analysis and Numerical Modeling, *Bull. Seism. Soc. Am.* **75**, 1395-1411.

Ewing, M. J., M. Jardetzky, and F. Press (1957). Elastic Waves in Layered Media, McGraw-Hill, New York.

Hansen, R., F. Ringdal, and P. Richards (1990). The Stability of RMS Lg Measurements and their Potential for Accurate Estimation of the Yields of Soviet Underground Nuclear Explosions, *Bull. Seism. Soc. Am.* **80**, 2106-2126.

Herrmann, R. (1980). Q Estimates using the Coda of Local Earthquakes, *Bull. Seism. Soc. Am.* **70**, 447-468.

Knopoff, L., P. Schwab, and E. Kausel (1973). Interpretation of Lg, *Geophys. J. R. Astr. Soc.* **33**, 389-404.

Menke, W. (1988). Geophysical Data Analysis: Discrete Inverse Theory, Academic Press, San Diego.

Nuttli, O. (1980). The Excitation and Attenuation of Seismic Crustal Phases in Iran, *Bull. Seism. Soc. Am.* **70**, 469-485.

Nuttli, O. (1986). Yield Estimates of Nevada Test Site Explosions Obtained from Seismic Lg Waves, *J. Geophys. Res.* **91**, 2137-2151.

Patton, H. J. (1988). Application of Nuttli's Method to Estimate Yield of Nevada Test Site Explosions Recorded on Lawrence Livermore National Laboratory's Digital Seismic System, *Bull. Seism. Soc. Am.* **78**, 1759-1772.

Rapine, R., J. Ni, and T. Hearn (1997). Regional Wave Propagation in China and Its Surrounding Regions, *Bull. Seism. Soc. Am.*, submitted.

Rodgers, A. J., T. Lay, W. R. Walter, and K. M. Mayeda (1997). Comparison of Regional Phase Amplitude Ratio Measurement Techniques, *Bull. Seism. Soc. Am.*, submitted.

Shin, T. and R. Herrmann (1987). Lg Attenuation and Source Studies Using 1982 Miramachi Data, *Bull. Seism. Soc. Am.* **77**, 384-397.

Wu, J., J. Ni, and T. Hearn (1996). Lg wave attenuation and propagation characteristics in Iran, in *Monitoring a Comprehensive Test Ban Treaty*, NATO ASI Vol., E. Husebye and A. Dainty (Editors), Kluwer Academic Publishers, 655-662.

Part II: Lateral variation of Pn and Lg propagation at CDSN Station LSA

2.1 Introduction

For continental paths, the regional phase Lg can be modeled successfully as the sum of higher mode surface waves or as a superposition of shear waves multiply reflected within the crustal waveguide with an approximate group velocity of 3.7 - 3.2 km/sec (Press and Ewing, 1952; Bouchon, 1982). The propagation of Lg is sensitive to the attenuation properties of the crust and heterogeneity of the crustal waveguide (Campillo, 1987; Husebye and Ruud, 1996). For regional distances, the phase Pn is the first arrival for event epicentral distances greater than about three degrees. The propagation of Pn can be modeled as a sum of whispering gallery waves in a sub-Moho waveguide made up of a high-velocity mantle lid over a low velocity zone (Menke and Richards, 1980). The shear wave counterpart to Pn is Sn. The group velocity of Pn is typically between 7.5 - 8.0 km/sec and varies with uppermost mantle temperature differences.

Many studies indicate that the attenuation of Lg is correlated with tectonic setting (Nuttli, 1986; Chavez and Priestly, 1986; Hasegawa, 1983; Atkinson and Mereu, 1992). In terms of a quality factor Q_{Lg}, low values of Q_{Lg} near one Hertz are indicative of tectonically active areas. On the other hand, stable areas such as cratons are typically characterized by large values of Q_{Lg} at one Hertz. Of course, in general, the quality factor is a function of frequency, $Q_{Lg} = Q_{Lg}(f)$. Areas of recent tectonism typically show strong frequency dependence of Q_{Lg} relative to stable areas. Upper mantle attenuation studies show that efficient wave propagation characterizes regions of low temperature, while large attenuation of the phases Sn and Pn is diagnostic of heating and partial melt in the upper mantle (Barazangi and Isacks, 1971; Kadinsky-Cade *et al.*, 1981; Whitman *et al.*, 1992).

The purpose of this study is to investigate lateral variation in the attenuation of Lg and Pn which propagate to the CDSN station LSA from epicentral distances out to 1200 km. The data are analyzed on an event by event basis to map azimuthal changes in the apparent attenuation

and correlate the variations with tectonics and surface geology. The attenuation of both Pn and Lg is characterized by a constant Q model for narrow frequency bands near one Hertz.

2.2 Method

The method for estimating lateral heterogenities in attenuation utilizes regional spectra from events with varying distances and azimuths. The analysis assumes a simple earthquake source spectrum uniquely characterized by the moment and a frequency independent, constant-Q model. The displacement amplitude spectrum of a signal arriving from a source at a distance r is

$$A(f,r) = S(f)\, I(f)\, G(r) \exp \frac{-\pi f r}{v_g Q} \tag{1}$$

where f is the frequency, v_g is the signal group velocity, S(f) is the source spectrum, I(f) is the instrument response, G(r) is the geometric spreading function, and the exponential term is the effective signal attenuation characterized by the quality factor Q. The attenuation of seismic signals involves both the absorption and scattering of energy. The quality factor in (1) is the sum of two terms representing the contributions of these two attenuation mechanisms and is sometimes called the apparent quality factor. The separation of attenuation into anelastic and scattering contributions is beyond the scope of this study. There are several effects which may influence the spectral amplitude which are not included in (1). The site response is known to depend strongly on local geology. In this study, the site response is assumed to be constant over the relatively narrow frequency bands considered. Additionally, the assumed source model spectrum does not include contributions from radiation pattern or source complexity. Although these effects are not explicitly included in (1), the simple spectral amplitude representation allows a self-consistent theoretical characterization of the lateral variation in the observed spectra.

The source spectra were assumed to have a simple form with a high frequency decay of f^{-2} above the corner frequency which scales with the inverse cube root of the moment,

$$S(f)=\frac{S_0}{1+f^2/f_c^2} \qquad f_c=kv_\beta\left(\frac{16\Delta\sigma}{7M_0}\right)^{1/3} \tag{2}$$

where S_0 is a constant, f_c is the corner frequency, k is a constant, v_β is the shear wave velocity at the source, $\Delta\sigma$ is the stress drop, and M_0 is the moment (Whitman *et. al.*, 1992; Brune, 1970). The moment was estimated from the moment magnitude scale log M_0 = 1.5 M_W + 16.1 with $M_W=m_b$ for the range of event magnitudes considered in this study (Hanks and Kanamori, 1979; Kanamori, 1983). The constant k ~ 0.33 for shear waves and k ~ 0.50 for compressional waves (Brune *et. al.*, 1979; *Molnar et. al.*, 1973). The stress drop was assumed to be 1 x 10^8 dyne/cm^2 and the shear wave velocity was taken to be the crustal average v_g = 3.5 km/sec. As in all spectral decay studies of attenuation, there is a trade-off between the assumed high frequency spectral roll-off and the attenuation derived from the observed spectral decay rate. A lower source roll off would yield lower values of Q while a higher spectral roll off would increase the Q estimate.

The observed displacement spectral amplitudes are corrected for instrument response and the source spectrum model. Using (1), the linear regression problem for Q is formulated as

$$\ln\left(\frac{D(f,r)}{I(f)}(1+f^2/f_c^2)\right)=\ln(S_0G(r))-\frac{\pi f r}{v_g Q} \tag{3}$$

where D(f,r) is the observed spectral amplitude. The logarithm of the corrected signal spectrum is a linear function of frequency. The first term on the right hand side controls the intercept while the coefficient on f involves Q. Thus, effective Q can be estimated by fitting a straight line to the observed corrected log spectrum.

2.3 Data

The data consist of event-triggered digital seismograms recorded at the CDSN station LSA, Lhasa, Tibet, from December, 1991 to August, 1995. The data were retrieved from the Incorporated Research Institutions for Seismology Data Management Center. The station was equipped with Streckeisen Model STS-1/VBB three component systems for the broadband, long period, and very long period data. The channel used for the calculation of propagation efficiency was the broadband vertical component BHZ. The data are digitally recorded at 20 samples per second. Event origin times, locations, and body wave magnitudes were taken from the Preliminary Determination of Epicenters catalog distributed by the U.S. Geological Survey. The location of the events used to calculate Pn and Lg spectra are shown in Figure 8 . The event epicenters are shown as circles and the location of the station LSA is shown as a triangle.

Regional spectra from events with epicentral distances between 200 and 1200 km and body wave magnitudes between 4.3 and 6.1 were calculated. In general, the data set provides fairly uniform azimuthal coverage. Azimuthal variations in Pn attenuation were estimated by inversion of 71 events for effective Q while 93 events were analyzed for Lg attenuation.

The Pn spectra were computed using a fixed time window of ten seconds beginning at the onset time of the arrival. A five percent Hanning taper was applied to the signal and to a pre-event noise sample. The resulting time series were zero padded to 256 samples and Fourier transformed. The noise power spectral density was subtracted from the signal power spectral density and the displacement spectral amplitude was estimated by correcting for the instrument response. The frequency band was selected on the basis of a signal-to-noise ratio of at least two. When the signal-to-noise ratio was sufficient for most of the frequency band but the signal had isolated spectral holes that fell below the noise level, a five point running average was used to smooth the signal spectrum near the spectral holes.

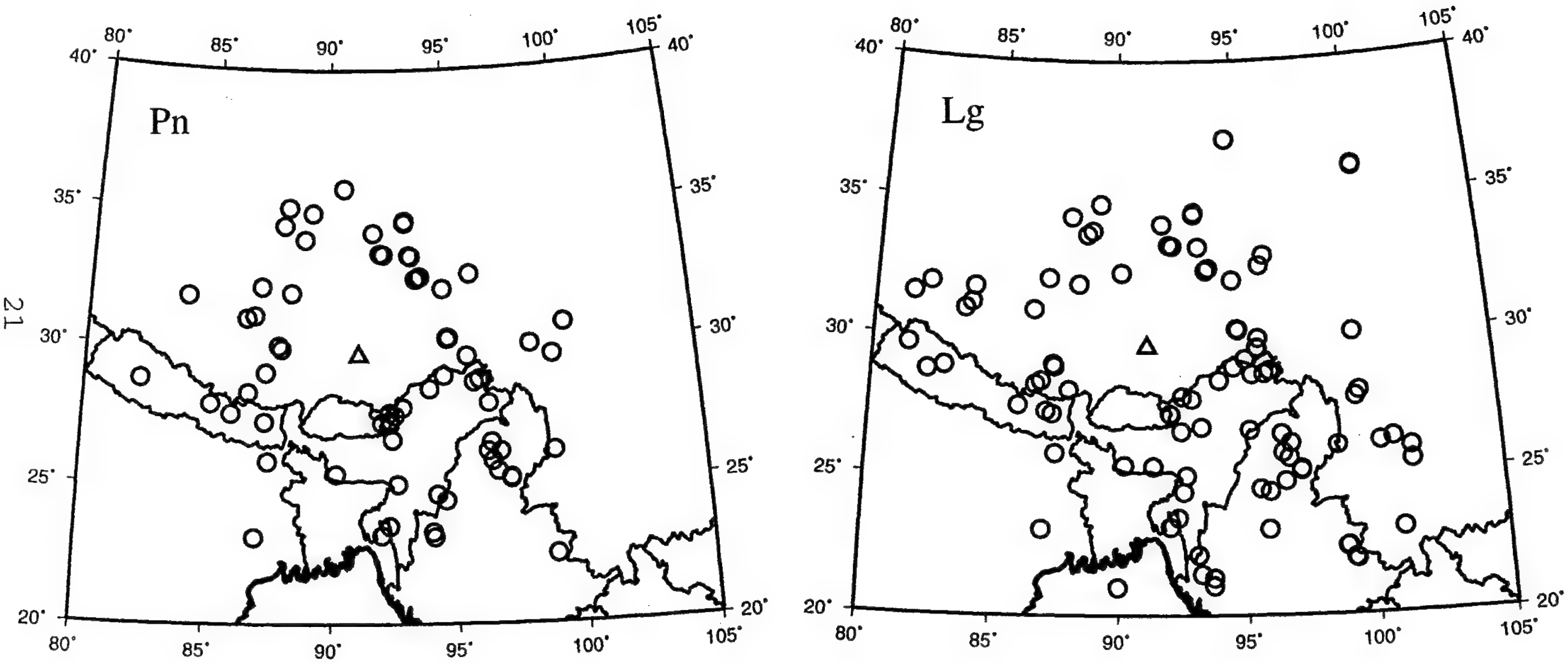

Figure 8.

The Lg spectra were computed from seismograms with a fixed group velocity window of 3.6 - 3.0 km/sec. A fixed velocity window was chosen so that the signal contained the same number of modes for all epicentral distances. This eliminates signal energy loss due to dispersion so that the estimated attenuation is due to absorption and scattering mechanisms only. The signal time series was zero padded to the nearest power of two. The resulting spectra were calculated and corrected for pre-event noise as in the Pn case.

The spectra were corrected for the source according to (3) and Q was calculated from a straight line fit to the corrected spectra for each event. If the source calculation overcorrected the observed spectra, resulting in negative values for Q, the corner frequency was postulated to lie above the frequency band used in the inversion. In this case, Q was calculated by assuming that $S(f) \sim S_0$ over the entire frequency band considered. The errors for the model attenuation estimates were found from the data kernel and the variance of the observed spectra.

2.4 Results

At distances greater than 1200 km the Lg signal is attenuated below the noise floor for frequencies greater than 3 Hz. Thus, the inversion for Lg was limited to frequencies between 0.5 and 3 Hz. The frequency band for Pn was between 0.5 and 4 Hz. In these relatively narrow frequency bands, the data admit a constant Q fit. Some examples of theoretical fits to Pn and Lg spectral data are shown in Figure 9. It should be noted, however, that in general Q is a function of frequency. This is especially important when trying to fit one attenuation model to data over a wide frequency band.

The apparent attenuation of both Lg and Pn exhibits strong azimuthal variation. The results of the calculation for effective Q are shown in Figure 10 as a function of event back azimuth. The error bars show plus and minus one standard deviation. In general, the attenuation is larger for events north of the station relative to events with southerly back azimuths for both Lg and Pn. The solid line is a least squares fit to a function of the form $A + B\cos\theta + C\sin\theta$, where θ

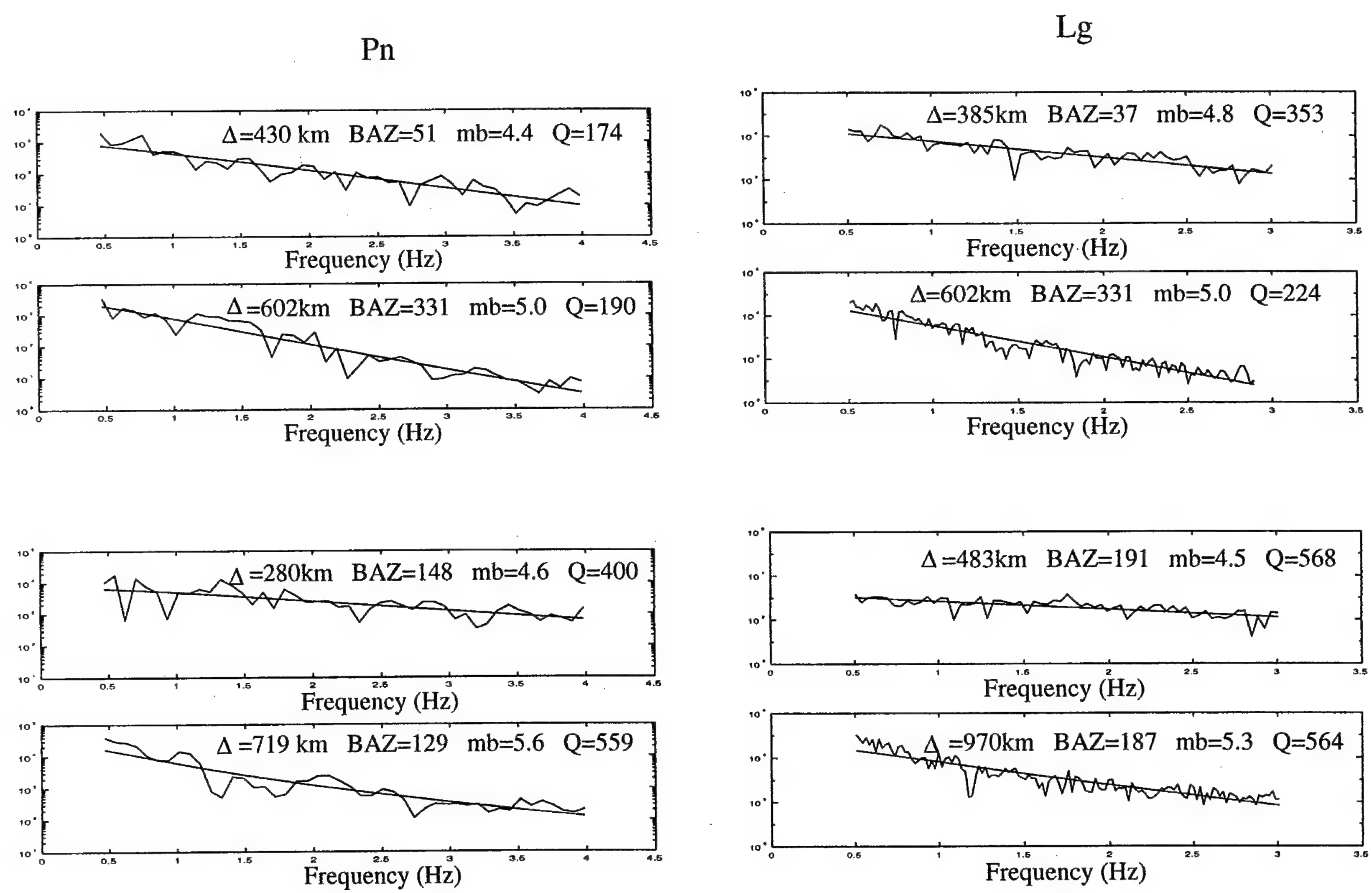

Pn
Lg
Δ=430 km BAZ=51 mb=4.4 Q=174
Δ=602km BAZ=331 mb=5.0 Q=190
Δ=280km BAZ=148 mb=4.6 Q=400
Δ=719 km BAZ=129 mb=5.6 Q=559
Δ=385km BAZ=37 mb=4.8 Q=353
Δ=602km BAZ=331 mb=5.0 Q=224
Δ=483km BAZ=191 mb=4.5 Q=568
Δ=970km BAZ=187 mb=5.3 Q=564
Frequency (Hz)

Figure 9.

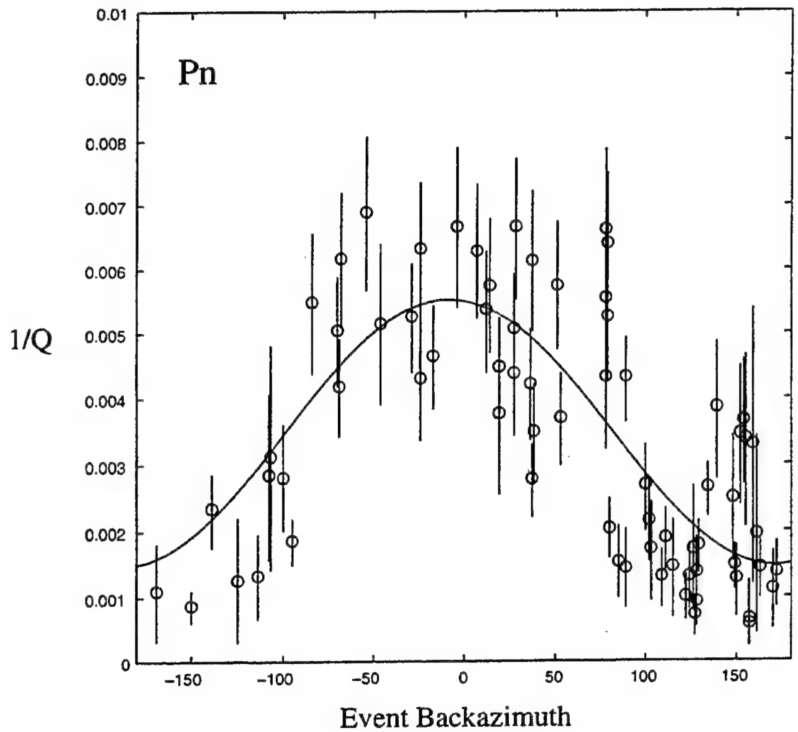

Pn
1/Q
0.01
0.009
0.008
0.007
0.006
0.005
0.004
0.003
0.002
0.001
0
-150
-100
-50
0
50
100
150
Event Backazimuth

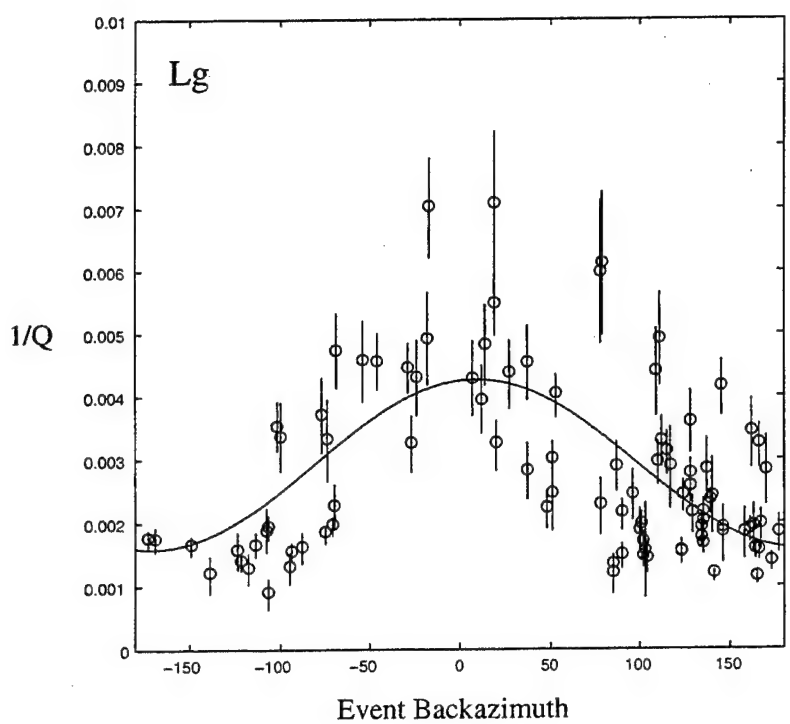

Lg
1/Q
0.01
0.009
0.008
0.007
0.006
0.005
0.004
0.003
0.002
0.001
0
-150
-100
-50
0
50
100
150
Event Backazimuth

Figure 10

is the back azimuth. These results indicate an effective attenuation of $Q_{Pn} \sim 240$ for northern raypaths and $Q_{Pn} \sim 670$ for southern raypaths. Likewise, the attenuation of the crustal phase Lg is characterized by $Q_{Lg} \sim 520$ for events north of the station and $Q_{Lg} \sim 340$ for southern events.

2.5 Discussion

The lateral variation in the transmission efficiency of Pn and Lg in the area considered in this study is consistent with previous observations. Regional Sn propagation efficiency was mapped qualitatively by Rapine *et al.* (1997). The authors found that for the station LSA, Sn propagates efficiently across the Himalayas and throughout southern Tibet, but is severely attenuated when crossing the north central portion of the Tibetan plateau. The same region of poor Sn propagation was observed by Ni and Barazangi (1983) and McNamara *et al.* (1995). This is consistent with the observations of low Q_{Pn} for events north of LSA and relatively high quality factors for southerly events. The observed strong Pn attenuation for events north of LSA can be explained by partial melt in the upper mantle. Partial melt may result from a mantle rich in crustal material due to past subduction events and the right temperature and pressure conditions. Water contained in the subducted lithosphere is released under appropriate conditions, effectively lowering the solidus temperature and enhancing partial melt. This interpretation was applied to the Iranian Plateau by Hearn and Ni (1994).

Likewise, Rapine *et al.* find that Lg signals generated by earthquakes in northern Tibet and observed at LSA exhibit large attenuation, while for southern events with raypaths perpendicular to the strike of the Himalayas, Lg transmission is efficient. The authors also show efficient Lg propagation from events to the southeast of LSA. This is consistent with the azimuthal variation observed in the Q_{Lg} values. It is widely observed that the boundaries of the Tibetan Plateau cause inefficient Lg propagation and even complete blockage of Lg. However, these observations were made at stations located far from the boundaries of the plateau. Stations near the boundaries of the plateau do record Lg for events outside the plateau. This indicates that Lg is scattered at the plateau boundaries and propagates some distance into the plateau before it is

completely attenuated. The results of this study are consistent with such observations and even indicate that at LSA, for the event epicentral distances considered, propagation across the southern boundary of the plateau is more efficient than propagation within the plateau itself.

2.6 Conclusion

Large lateral variations were observed for the attenuation of the regional phases Pn and Lg at the CDSN station LSA. These variations reflect the rheological properties of the uppermost mantle and the crust, respectively. It is evident that the complex geology of the region considered in this study has a significant effect on the propagation characteristics of high frequency regional seismic phases. It was generally observed that the propagation of both Pn and Lg within the Tibetan Plateau was less efficient than propagation across the southern boundary of the plateau.

The results of this study indicate that north of LSA, for events within the plateau, $Q_{Pn} \sim 240$ for frequencies near 1 Hz. For events south of LSA with raypaths crossing the Himalayan boundary thrust, $Q_{Pn} \sim 670$. This variation in Pn attenuation is most likely due to partial melt in the uppermost mantle beneath north central Tibet. Large S-P travel time residuals, blockage of Sn in the northern plateau, and basaltic and granitic volcanism at the surface all suggest that the upper mantle and crust beneath the northern plateau are hot (Molnar and Chen, 1984; Molnar, 1990; Ni and Barazangi, 1983). This observation is consistent with anomalously low Q_{Pn} values for raypaths from events within the plateau to LSA and low Pn velocities observed in the northern plateau by McNamara *et al.* (1995).

It has been suggested that the attenuation of Lg within the plateau may be due to a combination of factors including scattering at complex fault systems, low intrinsic Q due to crustal heating, and an increased path length associated with the thickness of the crust itself (McNamara *et al.*, 1996). This study indicates that for paths to LSA from events to the north, $Q_{Lg} \sim 340$. This value is indicative of tectonically active regions and is consistent with the values

of Q_{Lg} at 1 Hz, $Q_{Lg} \sim 366$ and $Q_{Lg} \sim 400$ found by McNamara *et al.* (1996) and Shih *et al.* (1994) for the plateau. For events to the south with raypaths crossing the southern boundary of the plateau, $Q_{Lg} \sim 520$, which is closer to values of Q measured in tectonically stable areas.

2.7 References

Atkinson, G.M. and R.F. Mereu (1992). The shape of ground motion attenuation curves in southeastern Canada, *Bull. Seism. Soc. Am.* **82**, 2014-2031.

Barazangi, M. and B. Isacks (1971). Lateral variations of seismic wave attenuation in the upper mantle above the inclined earthquake zone of the Tonga island arc: Deep anomaly in the upper mantle, *J. Geophys. Res.* **76**, 8493-8516.

Bouchon, M. (1982). The complete synthesis of seismic crustal phases at regional distances, *J. Geophys. Res.* **78**, 1735-1741.

Brune, J.N. (1970). Tectonic stress and the spectra of seismic shear waves from earthquake sources, *J. Geophys. Res.* **75**, 4997-5009.

Brune, J.N., R.J. Archuleta, and S. Hartzell (1979). Far-field S-wave spectra, corner frequencies, and pulse shapes, *J. Geophys. Res.* **84**, 2262-2272.

Campillo, M. (1987). Lg wave propagation in a laterally varying crust and the spatial distribution of the quality factor in central France, *J. Geophys. Res.* **92**, 12604-12614.

Chavez, D. and K. Priestley (1986). Measurements of frequency dependent Lg attenuation in the Great Basin, *Geophys. Res. Lett.* **13**, 551-554.

Hanks, T.C. and H. Kanamori (1979). A moment magnitude scale, *J. Geophys. Res.* **84**, 2348-2350.

Hasegawa, H. (1985). Attenuation of Lg waves in the Canadian Shield, *Bull. Seism. Soc. Am.* **75**, 1569-1582.

Hearn, T. and J. Ni (1994). Pn velocities beneath continental collision zones: the Turkish-Iranian Plateau, *Geophys. J. Int.* **117**, 273-283.

Husebye, E.S. and B.O. Ruud (1996). Wave propagation in a complex crust - CTBT implications, *Proceedings of the 18th Annual Seismic Research Symposium on Monitoring a Comprehensive Test Ban Treaty*, Phillips Laboratory, 172-181, PL-TR-96-2153, ADA313692.

Kadinsky-Cade, K., M. Barazangi, J. Oliver and B. Isacks (1981). Lateral variations of high-frequency seismic wave propagation at regional distances across the Turkish and Iranian plateau, *J. Geophys. Res.* **86**, 9377-9396.

Kanamori, H. (1983). Magnitude scale and quantification of earthquakes, *Tectonophysics* **93**, 185-199.

McNamara, D.E., T.J. Owens, and W.R. Walter (1995). Observations of regional phase propagation across the Tibetan Plateau, *J. Geophys. Res.* **100**, 22215-22229.

McNamara, D.E., T.J. Owens, and W.R. Walter (1996). Propagation Characteristics of Lg Across the Tibetan Plateau, *Bull. Seism. Soc. Am.* **86**, 457-469.

Menke, W.H., and P.G. Richards (1980). Crust-mantle whispering gallery phases: a deterministic model of teleseismic Pn wave propagation, *J. Geophys. Res.* **185**, 5416-5422.

Molnar, P. (1990). S-wave residuals from earthquakes in the Tibetan region and lateral variations in the upper mantle, *Earth Planet. Sci. Lett.* **101**, 68-77.

Molnar, P. and W.P. Chen (1984). S-P travel time residuals and lateral inhomogeneity in the mantle beneath Tibet and the Himalaya, *J. Geophys. Res.* **89**, 6911-6917.

Molnar, P., B.E. Tucker, and J.N. Brune (1973). Corner frequencies of P and S waves and models of earthquake sources, *Bull. Seism. Soc. Am.* **63**, 2091-2105.

Ni, J. and M. Barazangi (1983). Velocities and propagation characteristics of Pn, Pg, Sn and Lg seismic waves beneath the Indian Shield, Himalayan Arc, Tibetan Plateau, and surrounding regions: High uppermost mantle velocities and efficient Sn propagation beneath Tibet, *Geophys. J. R. Astr. Soc.* **72**, 665-689.

Nuttli, O. (1986). Yield estimates of Nevada test site explosions obtained from seismic Lg waves, *J. Geophys. Res.* **91**, 2137-2151.

Press, F. and M. Ewing (1952). Two Slow Surface Waves Across North America, *Bull. Seism. Soc. Am.* **42**, 219-228.

Rapine, R., J. Ni, and T. Hearn (1996). Regional wave propagation characteristics in the Middle East and southern China, *Sci. Rep. 1*, PL-TR-97-2030, Phillips Laboratory, Hanscom AFB, MA, ADA325890.

Shih, X.R., K.Y. Chun, and T. Zhu (1994). Attenuation of 1-6 s Lg waves in Eurasia, *J. Geophys. Res.* **99**, 23859-23874.

Whitman, D., B. Isacks, J.L. Chatelain, J.M. Chiu, and A. Perez (1992). Attenuation of high-frequency seismic waves beneath the Central Andean Plateau, *J. Geophys. Res.* **97**, 19929-19947.

THOMAS AHRENS
SEISMOLOGICAL LABORATORY 252-21
CALIFORNIA INST. OF TECHNOLOGY
PASADENA, CA 91125

AIR FORCE RESEARCH LABORATORY
ATTN: RESEARCH LIBRARY/TL
5 WRIGHT STREET
HANSCOM AFB, MA 01731-3004

RALPH ALEWINE
NTPO
1901 N. MOORE STREET, SUITE 609
ARLINGTON, VA 22209

G. Eli Baker
MAXWELL TECHNOLOGIES
8888 BALBOA AVE.
SAN DIEGO, CA 92123-1506

THERON J. BENNETT
MAXWELL TECHNOLOGIES
11800 SUNRISE VALLEY
SUITE 1212
RESTON, VA 22091

JONATHAN BERGER
UNIV. OF CALIFORNIA, SAN DIEGO
SCRIPPS INST. OF OCEANOGRAPHY IGPP, 0225
9500 GILMAN DRIVE
LA JOLLA, CA 92093-0225

LESLIE A. CASEY
DEPT. OF ENERGY/NN-20
1000 INDEPENDENCE AVE. SW
WASHINGTON DC 20585-0420

ANTON DAINTY
HQ DSWA/PMA
6801 TELEGRAPH ROAD
ALEXANDRIA, VA 22310-3398

DIANE DOSER
DEPT. OF GEOLOGICAL SCIENCES
THE UNIVERSITY OF TEXAS AT EL PASO
EL PASO, TX 79968

MARK D. FISK
MISSION RESEARCH CORPORATION
735 STATE STREET
P.O. DRAWER 719
SANTA BARBARA, CA 93102-0719

AIR FORCE RESEARCH LABORATORY
ATTN: VSOE
29 RANDOLPH ROAD
HANSCOM AFB, MA 01731-3010 (2 COPIES)

AIR FORCE RESEARCH LABORATORY
ATTN: AFRL/SUL
3550 ABERDEEN AVE SE
KIRTLAND AFB, NM 87117-5776 (2 COPIES)

MUAWIA BARAZANGI
INSTOC
3126 SNEE HALL
CORNELL UNIVERSITY
ITHACA, NY 14853

DOUGLAS BAUMGARDT
ENSCO INC.
5400 PORT ROYAL ROAD
SPRINGFIELD, VA 22151

WILLIAM BENSON
NAS/COS
ROOM HA372
2001 WISCONSIN AVE. NW
WASHINGTON DC 20007

ROBERT BLANDFORD
AFTAC
1300 N. 17TH STREET
SUITE 1450
ARLINGTON, VA 22209-2308

CENTER FOR MONITORING RESEARCH
ATTN: LIBRARIAN
1300 N. 17th STREET, SUITE 1450
ARLINGTON, VA 22209

CATHERINE DE GROOT-HEDLIN
UNIV. OF CALIFORNIA, SAN DIEGO
IGPP
8604 LA JOLLA SHORES DRIVE
SAN DIEGO, CA 92093

DTIC
8725 JOHN J. KINGMAN ROAD
FT BELVOIR, VA 22060-6218 (2 COPIES)

LORI GRANT
MULTIMAX, INC.
311C FOREST AVE. SUITE 3
PACIFIC GROVE, CA 93950

HENRY GRAY
SMU STATISTICS DEPARTMENT
P.O. BOX 750302
DALLAS, TX 75275-0302

I. N. GUPTA
MULTIMAX, INC.
1441 MCCORMICK DRIVE
LARGO, MD 20774

DAVID HARKRIDER
BOSTON COLLEGE
INSTITUTE FOR SPACE RESEARCH
140 COMMONWEALTH AVENUE
CHESTNUT HILL, MA 02167

THOMAS HEARN
NEW MEXICO STATE UNIVERSITY
DEPARTMENT OF PHYSICS
LAS CRUCES, NM 88003

MICHAEL HEDLIN
UNIVERSITY OF CALIFORNIA, SAN DIEGO
SCRIPPS INST. OF OCEANOGRAPHY
9500 GILMAN DRIVE
LA JOLLA, CA 92093-0225

DONALD HELMBERGER
CALIFORNIA INST. OF TECHNOLOGY
DIV. OF GEOL. & PLANETARY SCIENCES
SEISMOLOGICAL LABORATORY
PASADENA, CA 91125

EUGENE HERRIN
SOUTHERN METHODIST UNIVERSITY
DEPT. OF GEOLOGICAL SCIENCES
DALLAS, TX 75275-0395

ROBERT HERRMANN
ST. LOUIS UNIVERSITY
DEPT. OF EARTH & ATMOS. SCIENCES
3507 LACLEDE AVENUE
ST. LOUIS, MO 63103

VINDELL HSU
HQ/AFTAC/TTR
1030 S. HIGHWAY A1A
PATRICK AFB, FL 32925-3002

RONG-SONG JIH
HQ DSWA/PMA
6801 TELEGRAPH ROAD
ALEXANDRIA, VA 22310-3398

THOMAS JORDAN
MASS. INST. OF TECHNOLOGY
BLDG 54-918
CAMBRIDGE, MA 02139

LAWRENCE LIVERMORE NAT'L LAB
ATTN: TECHNICAL STAFF (PLS ROUTE)
PO BOX 808, MS L-175
LIVERMORE, CA 94551

LAWRENCE LIVERMORE NAT'L LAB
ATTN: TECHNICAL STAFF (PLS ROUTE)
PO BOX 808, MS L-208
LIVERMORE, CA 94551

LAWRENCE LIVERMORE NAT'L LAB
ATTN: TECHNICAL STAFF (PLS ROUTE)
PO BOX 808, MS L-202
LIVERMORE, CA 94551

LAWRENCE LIVERMORE NAT'L LAB
ATTN: TECHNICAL STAFF (PLS ROUTE)
PO BOX 808, MS L-195
LIVERMORE, CA 94551

LAWRENCE LIVERMORE NAT'L LAB
ATTN: TECHNICAL STAFF (PLS ROUTE)
PO BOX 808, MS L-205
LIVERMORE, CA 94551

LAWRENCE LIVERMORE NAT'L LAB
ATTN: TECHNICAL STAFF (PLS ROUTE)
PO BOX 808, MS L-200
LIVERMORE, CA 94551

LAWRENCE LIVERMORE NAT'L LAB
ATTN: TECHNICAL STAFF (PLS ROUTE)
PO BOX 808, MS L-221
LIVERMORE, CA 94551

THORNE LAY
UNIV. OF CALIFORNIA, SANTA CRUZ
EARTH SCIENCES DEPARTMENT
EARTH & MARINE SCIENCE BUILDING
SANTA CRUZ, CA 95064

ANATOLI L. LEVSHIN
DEPARTMENT OF PHYSICS
UNIVERSITY OF COLORADO
CAMPUS BOX 390
BOULDER, CO 80309-0309

JAMES LEWKOWICZ
WESTON GEOPHYSICAL CORP.
325 WEST MAIN STREET
NORTHBORO, MA 01532

LOS ALAMOS NATIONAL LABORATORY
ATTN: TECHNICAL STAFF (PLS ROUTE)
PO BOX 1663, MS F659
LOS ALAMOS, NM 87545

LOS ALAMOS NATIONAL LABORATORY
ATTN: TECHNICAL STAFF (PLS ROUTE)
PO BOX 1663, MS F665
LOS ALAMOS, NM 87545

LOS ALAMOS NATIONAL LABORATORY
ATTN: TECHNICAL STAFF (PLS ROUTE)
PO BOX 1663, MS C335
LOS ALAMOS, NM 87545

GARY MCCARTOR
SOUTHERN METHODIST UNIVERSITY
DEPARTMENT OF PHYSICS
DALLAS, TX 75275-0395

KEITH MCLAUGHLIN
CENTER FOR MONITORING RESEARCH
SAIC
1300 N. 17TH STREET, SUITE 1450
ARLINGTON, VA 22209

BRIAN MITCHELL
DEPARTMENT OF EARTH & ATMOSPHERIC SCIENCES
ST. LOUIS UNIVERSITY
3507 LACLEDE AVENUE
ST. LOUIS, MO 63103

RICHARD MORROW
USACDA/IVI
320 21ST STREET, N.W.
WASHINGTON DC 20451

JOHN MURPHY
MAXWELL TECHNOLOGIES
11800 SUNRISE VALLEY DRIVE
SUITE 1212
RESTON, VA 22091

JAMES NI
NEW MEXICO STATE UNIVERSITY
DEPARTMENT OF PHYSICS
LAS CRUCES, NM 88003

ROBERT NORTH
CENTER FOR MONITORING RESEARCH
1300 N. 17th STREET, SUITE 1450
ARLINGTON, VA 22209

OFFICE OF THE SECRETARY OF DEFENSE
DDR&E
WASHINGTON DC 20330

JOHN ORCUTT
INST. OF GEOPH. & PLANETARY PHYSICS
UNIV. OF CALIFORNIA, SAN DIEGO
LA JOLLA, CA 92093

PACIFIC NORTHWEST NAT'L LAB
ATTN: TECHNICAL STAFF (PLS ROUTE)
PO BOX 999, MS K6-48
RICHLAND, WA 99352

PACIFIC NORTHWEST NAT'L LAB
ATTN: TECHNICAL STAFF (PLS ROUTE)
PO BOX 999, MS K6-40
RICHLAND, WA 99352

PACIFIC NORTHWEST NAT'L LAB
ATTN: TECHNICAL STAFF (PLS ROUTE)
PO BOX 999, MS K6-84
RICHLAND, WA 99352

PACIFIC NORTHWEST NAT'L LAB
ATTN: TECHNICAL STAFF (PLS ROUTE)
PO BOX 999, MS K5-12
RICHLAND, WA 99352

FRANK PILOTTE
HQ AFTAC/TT
1030 S. HIGHWAY A1A
PATRICK AFB, FL 32925-3002

KEITH PRIESTLEY
DEPARTMENT OF EARTH SCIENCES
UNIVERSITY OF CAMBRIDGE
MADINGLEY RISE, MADINGLEY ROAD
CAMBRIDGE, CB3 OEZ UK

JAY PULLI
BBN SYSTEMS AND TECHNOLOGIES, INC.
1300 NORTH 17TH STREET
ROSSLYN, VA 22209

DELAINE REITER
AFRL/VSOE (SENCOM)
73 STANDISH ROAD
WATERTOWN, MA 02172

MICHAEL RITZWOLLER
DEPARTMENT OF PHYSICS
UNIVERSITY OF COLORADO
CAMPUS BOX 390
BOULDER, CO 80309-0309

CHANDAN SAIKIA
WOOODWARD-CLYDE FED. SERVICES
566 EL DORADO ST., SUITE 100
PASADENA, CA 91101-2560

SANDIA NATIONAL LABORATORY
ATTN: TECHNICAL STAFF (PLS ROUTE)
DEPT. 9311
MS 1159, PO BOX 5800
ALBUQUERQUE, NM 87185-1159

SANDIA NATIONAL LABORATORY
ATTN: TECHNICAL STAFF (PLS ROUTE)
DEPT. 5736
MS 0655, PO BOX 5800
ALBUQUERQUE, NM 87185-0655

AVI SHAPIRA
SEISMOLOGY DIVISION
IPRG
P.O.B. 2286 NOLON 58122 ISRAEL

MATTHEW SIBOL
ENSCO, INC.
445 PINEDA CT.
MELBOURNE, FL 32940

JEFFRY STEVENS
MAXWELL TECHNOLOGIES
8888 BALBOA AVE.
SAN DIEGO, CA 92123-1506

TACTEC
BATTELLE MEMORIAL INSTITUTE
505 KING AVENUE
COLUMBUS, OH 43201 (FINAL REPORT)

LAWRENCE TURNBULL
ACIS
DCI/ACIS
WASHINGTON DC 20505

PAUL RICHARDS
COLUMBIA UNIVERSITY
LAMONT-DOHERTY EARTH OBSERV.
PALISADES, NY 10964

DAVID RUSSELL
HQ AFTAC/TTR
1030 SOUTH HIGHWAY A1A
PATRICK AFB, FL 32925-3002

SANDIA NATIONAL LABORATORY
ATTN: TECHNICAL STAFF (PLS ROUTE)
DEPT. 5704
MS 0979, PO BOX 5800
ALBUQUERQUE, NM 87185-0979

SANDIA NATIONAL LABORATORY
ATTN: TECHNICAL STAFF (PLS ROUTE)
DEPT. 5704
MS 0655, PO BOX 5800
ALBUQUERQUE, NM 87185-0655

THOMAS SERENO JR.
SAIC
10260 CAMPUS POINT DRIVE
SAN DIEGO, CA 92121

ROBERT SHUMWAY
410 MRAK HALL
DIVISION OF STATISTICS
UNIVERSITY OF CALIFORNIA
DAVIS, CA 95616-8671

DAVID SIMPSON
IRIS
1200 NEW YORK AVE., NW
SUITE 800
WASHINGTON DC 20005

BRIAN SULLIVAN
BOSTON COLLEGE
INSITUTE FOR SPACE RESEARCH
140 COMMONWEALTH AVENUE
CHESTNUT HILL, MA 02167

NAFI TOKSOZ
EARTH RESOURCES LABORATORY
M.I.T.
42 CARLTON STREET, E34-440
CAMBRIDGE, MA 02142

GREG VAN DER VINK
IRIS
1200 NEW YORK AVE., NW
SUITE 800
WASHINGTON DC 20005

FRANK VERNON
UNIV. OF CALIFORNIA, SAN DIEGO
SCRIPPS INST. OF OCEANOGRAPHY
9500 GILMAN DRIVE
LA JOLLA, CA 92093-0225

TERRY WALLACE
UNIVERSITY OF ARIZONA
DEPARTMENT OF GEOSCIENCES
BUILDING #77
TUCSON, AZ 85721

JILL WARREN
LOS ALAMOS NATIONAL LABORATORY
GROUP NIS-8
P.O. BOX 1663
LOS ALAMOS, NM 87545 (5 COPIES)

DANIEL WEILL
NSF
EAR-785
4201 WILSON BLVD., ROOM 785
ARLINGTON, VA 22230

RU SHAN WU
UNIV. OF CALIFORNIA, SANTA CRUZ
EARTH SCIENCES DEPT.
1156 HIGH STREET
SANTA CRUZ, CA 95064

JIAKANG XIE
COLUMBIA UNIVERSITY
LAMONT DOHERTY EARTH OBSERV.
ROUTE 9W
PALISADES, NY 10964

JAMES E. ZOLLWEG
BOISE STATE UNIVERSITY
GEOSCIENCES DEPT.
1910 UNIVERSITY DRIVE
BOISE, ID 83725